GRAPHENE AND 2DM VIRTUAL CONFERENCE & EXPO

Graphene online 2020 October 19-23

Moiré superlattice effects and band structure evolution in near-30-degree twisted bilayer graphene

M. J. Hamer[1,2], A. Giampietri[3], V. Kandyba[3], F. Genuzio[3], A. Locatelli[3], R. V. Gorbachev[1,2,4], A. V. Barinov[3], and M. Mucha-Kruczynski[5,6]

1 *Department of Physics, University of Manchester, Oxford Road, Manchester, M13 9PL, United Kingdom*
2 *National Graphene Institute, University of Manchester, Booth Street East, Manchester, M13 9PL, United Kingdom*
3 *Elettra-Sincrotrone Trieste ScPA, Trieste 34149, Italy*
4 *Henry Royce Institute, Oxford Road, Manchester, M13 9PL, United Kingdom*
5 *Department of Physics, University of Bath, Claverton Down, Bath BA2 7AY, United Kingdom*
6 *Centre for Nanoscience and Nanotechnology, University of Bath, Claverton Down, Bath BA2 7AY, United Kingdom*

In stacks of two-dimensional crystals, mismatch of their lattice constants and misalignment of crystallographic axes lead to formation of moiré patterns. We show that moiré superlattice effects persist in twisted bilayer graphene with large twists and short moiré periods. Using angle-resolved photoemission spectroscopy, we observe changes in valence band topology across large parts of the graphene Brillouin zone, including vicinity of the saddle point at ***M*** and across over 3 eV from the Dirac points. We also detect signatures of potential secondary Dirac points in the reconstructed dispersions. For twists $\theta > 21.8°$, Umklapp scattering of electrons in one graphene layer on the potential of the other leads to intervalley coupling and minigaps at energies above the gap due to cone anti-crossing, usually considered the only low-energy feature due to interlayer coupling. Our work showcases the potential to engineer electronic dispersions of stacks of two-dimensional crystals by tuning the interface twist angles. Our results demonstrate how, in a stack of two-dimensional crystals, the twist angle at an interface between two of the layers can be used to modify the electronic dispersion of the structure through a variety of mechanisms across a large range of θ.

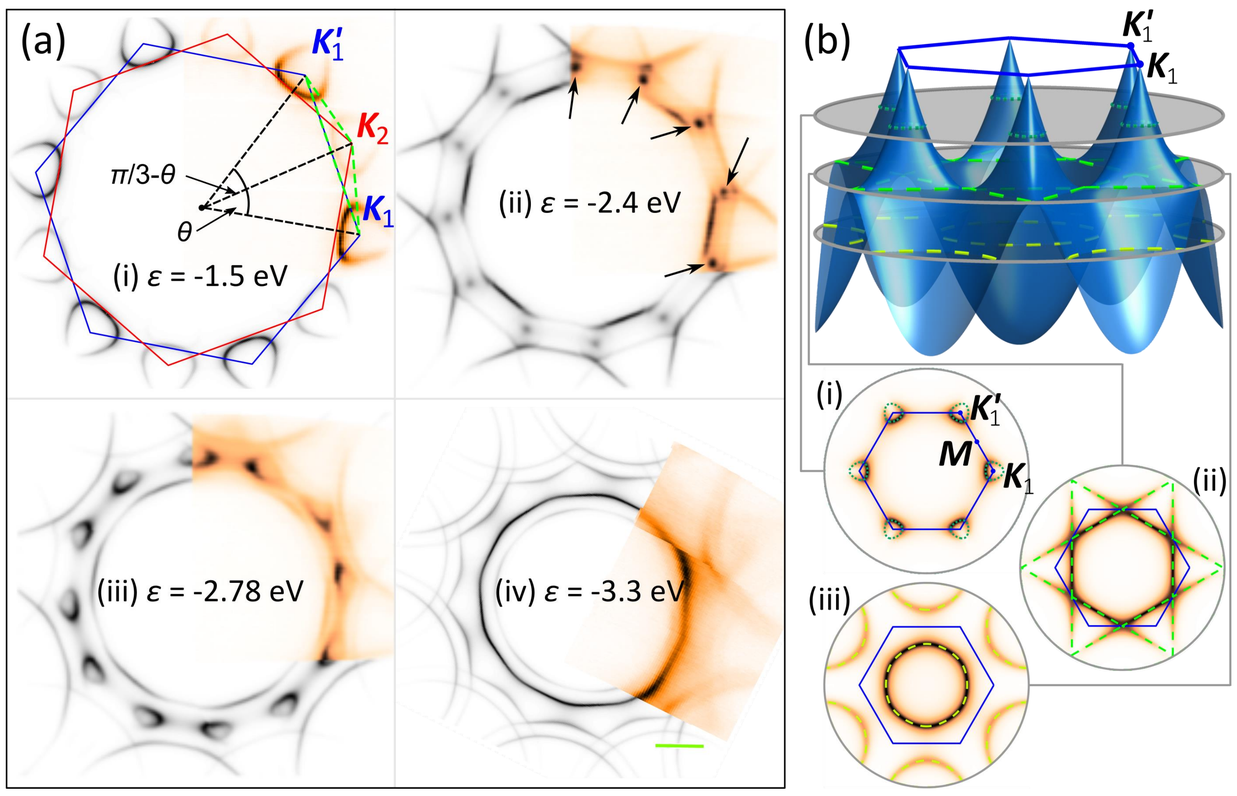

Fig. 1: Topology of energy contours in tBLG. (a) ARPES constant-energy maps of sample with $\theta = 29.7°$; experimental data is shown in colour and theoretical simulation in black and white. The blue and red hexagons show Brillouin zones of the top ($i = 1$) and bottom ($i = 2$) layers, respectively, and the green dashed line indicates the path in *k*-space for cuts in Fig. 3(b). $\boldsymbol{K_i}$ and $\boldsymbol{K_i'}$ denote the inequivalent Brillouin zone corners of layer i. Arrows in panel (ii) point to extrema of new minibands which harbour secondary Dirac points. All panels show the same *k*-space area and the green scale bar in (iv) corresponds to 0.5 A^{-1}. (b) Top: valence band of monolayer graphene and its characteristic cross sections. The jade green, bright green and yellow lines show energy contours for cuts indicated by gray planes. Bottom: simulated monolayer graphene ARPES constant-energy maps at energies of the cuts above. The saddle points in monolayer graphene dispersion are located at ***M***.

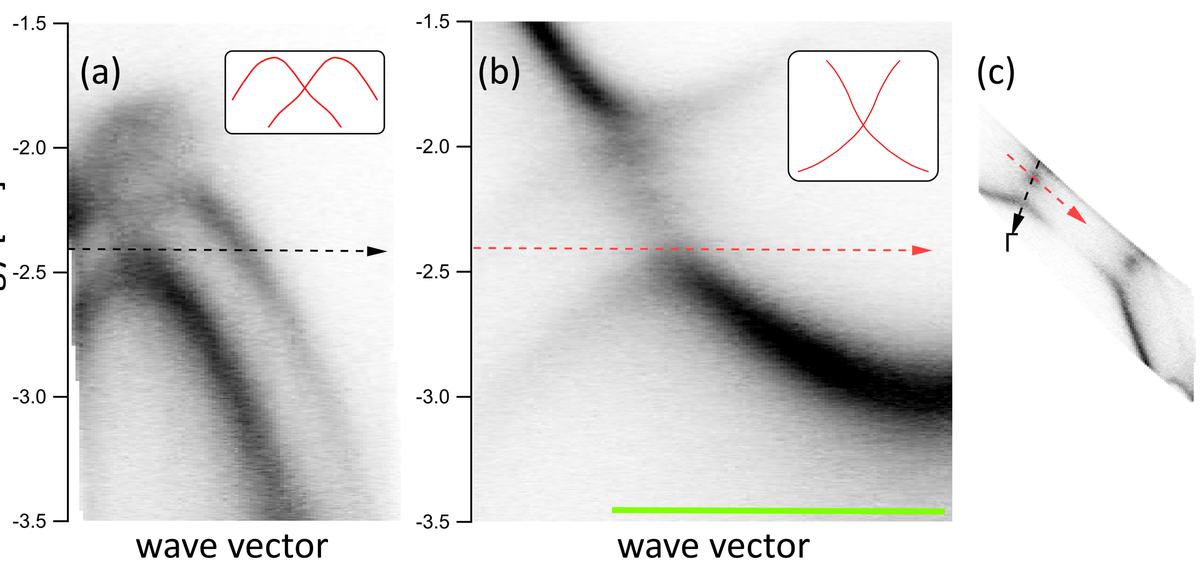

Fig, 2: Possible secondary Dirac point in the miniband spectrum of large-twist tBLG. (a), (b) show *k*-space cuts through one of the points indicated with black arrows in Fig. 1 along directions shown in (c). The insets show our interpretation of the miniband dispersion around the energy $\varepsilon \approx -2.4$ eV. The green scale bar corresponds to 0.5 A^{-1}. (c) Section of the ARPES constant-energy map at $\varepsilon \approx -2.4$ eV showing positions of cuts in (a) and (b). The black arrow is directed towards the $\boldsymbol{\Gamma}$ point.

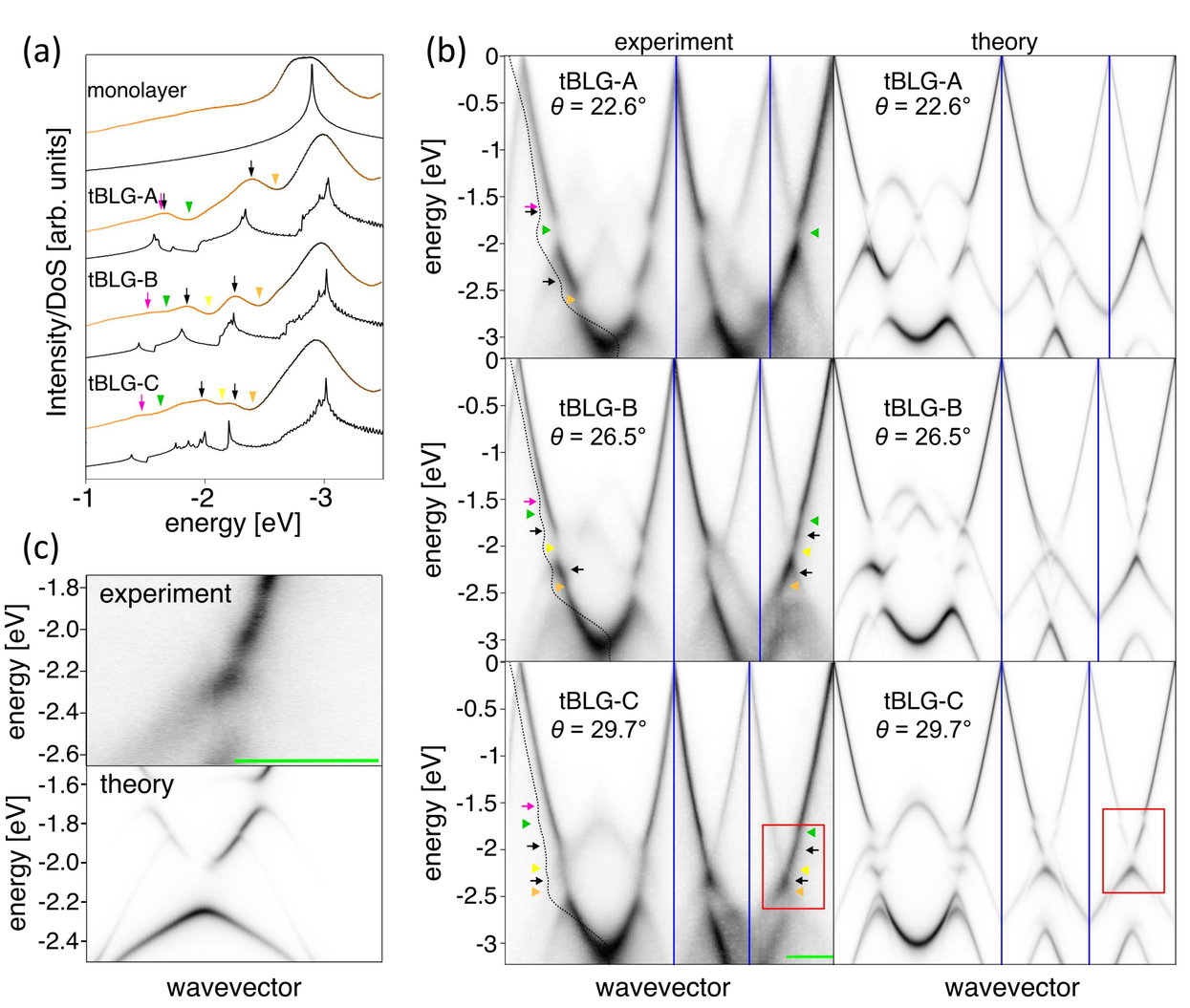

Fig. 3: Minigaps in large-angle tBLG. (a) Energy distribution curves and simulated electronic density of states (DoS) for monolayer graphene and our tBLG devices. Arrows and triangles indicate positions of van Hove singularities (vHs) and minigaps with colours differentiating between the origin of the features as discussed in the text. (b) ARPES intensity along *k*-space path shown with green dashed line in Fig. 1(a), together with the corresponding theoretical simulation (right). (c) Closeup of the area marked with the red rectangle in (b). The green scale bars in (b) and (c) correspond to 0.5 A^{-1}.

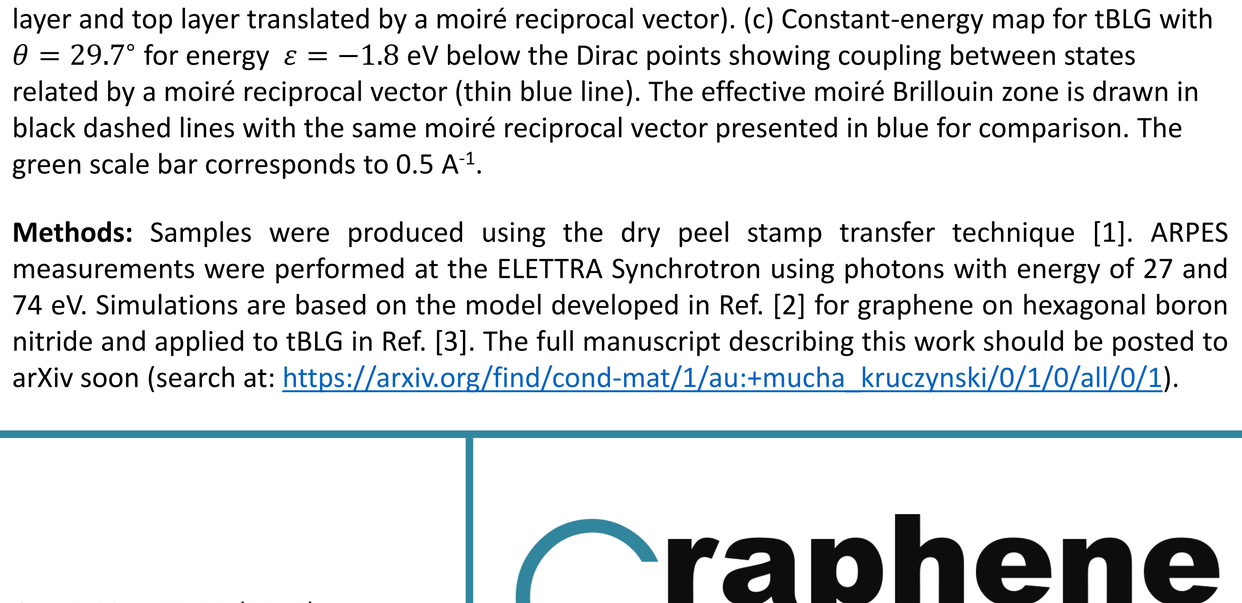

Fig. 4: Umklapp scattering in large-angle tBLG. (a) Evolution of the tBLG DoS for $\theta = 2°$ (red) to $\theta = 30°$ (blue), in steps of 1° (curves have been shifted vertically for clarity). The dashed lines are guides for the eye indicating, for given θ, highest energies of the crossings marked with the corresponding colour in (b). (b) Hierarchy of crossings in tBLG with $\theta > 21.8°$. The blue and red hexagons are the Brillouin zones of the top and bottom graphene layer and the corresponding valence band structures in the vicinity of $\boldsymbol{K_1}$, $\boldsymbol{K_1'}$ and $\boldsymbol{K_2}$ are shown with blue and red surfaces. The cyan cone depicts the $\boldsymbol{K_1'}$ states shifted by a moiré reciprocal vector indicated with the cyan arrow (the moiré Brillouin zone is shown in gray). Crossings between monolayer graphene dispersions are highlighted in black (between two graphene dispersions twisted by θ), magenta (original top layer dispersion and that translated by a moiré reciprocal vector) and white (bottom layer and top layer translated by a moiré reciprocal vector). (c) Constant-energy map for tBLG with $\theta = 29.7°$ for energy $\varepsilon = -1.8$ eV below the Dirac points showing coupling between states related by a moiré reciprocal vector (thin blue line). The effective moiré Brillouin zone is drawn in black dashed lines with the same moiré reciprocal vector presented in blue for comparison. The green scale bar corresponds to 0.5 A^{-1}.

Methods: Samples were produced using the dry peel stamp transfer technique [1]. ARPES measurements were performed at the ELETTRA Synchrotron using photons with energy of 27 and 74 eV. Simulations are based on the model developed in Ref. [2] for graphene on hexagonal boron nitride and applied to tBLG in Ref. [3]. The full manuscript describing this work should be posted to arXiv soon (search at: https://arxiv.org/find/cond-mat/1/au:+mucha_kruczynski/0/1/0/all/0/1).

CONTACT PERSON

Marcin Mucha-Kruczynski
mlmk20@bath.ac.uk

REFERENCES

[1] R. Frisenda *et al.*, Chemical Society Reviews **47**, 53 (2018).
[2] M. Mucha-Kruczynski, J. R. Wallbank, and V. I. Fal'ko, Physical Review B **93**, 085409 (2016).
[3] J. J. P. Thompson *et al.*, Nature Communications **11**, 3582 (2020).

Graphene online 2020